Scientific Research Publishing

Journal of Applied Mathematics and Physics, 2024, 12, 3923-3940
https://www.scirp.org/journal/jamp
ISSN Online: 2327-4379
ISSN Print: 2327-4352

Mathematical Modeling for Optimizing the Structural Properties of Catalysts Used for Series Multiple Reactions

Violeta Martínez[1], Farhang Shadman[2]

[1]Departamento de Ingeniería de Procesos y Ciencias Ambientales, Universidad Centroamericana "José Simeón Cañas", El Salvador, San Salvador
[2]Department of Chemical and Environmental Engineering, University of Arizona, Tucson, AZ, USA
Email: vamartinez@uca.edu.sv

How to cite this paper: Martínez, V. and Shadman, F. (2024) Mathematical Modeling for Optimizing the Structural Properties of Catalysts Used for Series Multiple Reactions. *Journal of Applied Mathematics and Physics*, **12**, 3923-3940.
https://doi.org/10.4236/jamp.2024.1211239

Received: October 21, 2024
Accepted: November 25, 2024
Published: November 28, 2024

Abstract

One of the main challenges in the design and operation of catalytic reactors for reactions with multiple paths/steps is the occurrence of undesirable reactions and products. In these cases, two main factors need to be considered in the reactor performance: the "conversion" of the feed and the "selectivity" of the process, which is the conversion split between the desired and the undesired products. In this work, a comprehensive model is developed and used to assess the impact of pore-size distribution (PSD) on both conversion and selectivity in series catalytic reactions. In particular, the evaluation considers the effects of various combinations of micro- and macro-porosity, the potential advantages of radial variation of the porosity in the catalyst pellets, and the effect of pellet size. Results show that, for series reactions, when the formation of the desired product is followed by an undesirable degradation reaction, higher porosity in pellets, particularly in the micro-range, gives higher overall conversion, but lowers selectivity towards the formation of the desired product. Selectivity in these pellets can be improved by using a non-uniform PSD that provides a radial gradient of effective diffusivity in pellets increasing from the center to the outer pellet surface. The pellet size also has a significant effect, and larger pellets show lower selectivity in most cases. In general, conversion and selectivity trends move in opposite directions with changes in PSD and the pore structural properties of pellets. Therefore, finding the optimum design of pellets is an optimization process that requires process modeling. Consequently, selecting the best catalyst properties involves optimization, and the needed tool is a comprehensive mathematical model that takes into account the details of mass transport and reaction kinetics in the catalyst pellets. Our primary objective has been the development of a flexible mathematical model that would be applicable to a wide range of conditions and can be used as a design tool and an optimization platform.

Keywords

Series Catalytic Reactions, Process Simulation, Pore-Size Distribution, Selectivity, Non-Uniform Catalyst Pellets

1. Introduction

One of the challenges in the design and operation of catalytic reactors is that the desired reactions for the production of a compound are often accompanied by undesirable reactions that occur simultaneously. The undesired reactions produce compounds that are wasteful and lower the performance of the reactor. There are various examples of this situation in hydrocarbon processing, such as hydrogenation, dehydrogenation, and cracking, when multiple reactions complicate the process [1]-[7]. The undesirable reaction path can be in parallel or in series with the main reaction. In these cases, two main factors need to be considered in the evaluation of the reactor performance for multiple reactions: the "conversion" of the feed, which is defined as the fraction of the main feed to the reactor that is converted to one or all of the products, and the "selectivity", which shows the split between the desired and the undesired products and is defined as the fraction of the conversion that goes into desired product [8]. Designs for such processes should not only aim at maximizing both the feed conversion and the reaction selectivity.

The issue of conversion and selectivity is particularly important in many series types of industrial catalytic reactions. In these reactions, the initial step (initial part of the series reaction) leads to the production of the desirable product, but the continuation of the reaction (later part of the reaction) causes the degradation of the desired product into undesirable waste compounds. This phenomenon is common in many hydrocarbon-processing catalytic reactions, such as hydrogenation, dehydrogenation, isomerization, and cracking [5] [9]-[13]. Maximizing both selectivity and conversion is critical but often a complex design and optimization challenge. The choice of catalyst material and chemistry is clearly one factor. However, since the heterogeneous catalytic reactions are influenced by mass transport into catalyst pellets, the transport steps also have significant effects on both conversion and selectivity. In fact, this transport influence can become a large and even dominating factor in many cases and a practical way for fine-tuning the reactor performance.

The main transport resistance in the reactions on typical porous catalyst pellets is what is called intra-phase transport, which involves various mechanisms of diffusion inside the pores of the catalyst pellets. This transport strongly depends on pore structure properties such as porosity and pore size distribution [14]. Given the substantial progress in the synthesis of porous catalysts [15]-[24], it is possible to utilize the selection and the structural properties of pores in the pellets, such as pore-size distribution (PSD), as a tool for increasing both the overall production

rate and the selectivity in dealing with multiple reactions.

The effect of pore size and its distribution within the catalyst pellets on the heterogeneous reactions have been the subject of a number of previous studies [25]. Some of these studies have investigated the effects of spatial distributions of pore size and porosity on reactions [18] [25]-[29]. However, there is a need for a comprehensive process model as a versatile tool to capture the effect of PSD on the performance features of multiple reactions. For example, in the work of Zhu *et al.* (2018), the pore size and porosity were continuously varied from the external pellet surface to the core to evaluate the effect on the performance of the methanol-to-olefin porous catalyst pellet. The results of this study showed that smaller pore diameters favor the process. In a similar work, Wang & Coppens (2008) found that the introduction of macropores into a mesoporous catalytic material increases the catalytic activity for one-step first-order reactions, and some others reported that uniform PSD is optimal under those conditions [30] [31].

In general, assessing the impact of PSD at the industrial scale is not practical due to the high cost of equipment and manpower, plus major interruption and impact on the operation if attempted in an existing facility. This assessment, at least for feasibility and trend studies, is preferred and more feasible by process simulation [32]-[39]. Additionally, process modeling is a more effective method compared to the trial-and-error approach that is sometimes used for catalyst selection and development [38]-[42]. In many cases, process modeling is the only feasible and practical way of investigating the trends prior to the more detailed fine-tuning of the process.

A primary goal of this study has been to develop a general and comprehensive model that includes the key performance features of the process (conversion and selectivity) and provides the flexibility to use various kinetics and multiple reactions, as well as the intra-phase transport effects and the pore structure and distribution parameters. In particular, the focus of the present work has been on the effect of PSD on a class of series reactions where the desired product is produced in the first part of the process. In the second part of the series reactions, this product can undergo degradation, producing undesirable waste. Examples of this case are hydrogenation, dehydrogenation, and various hydrocarbon processing reactions such as cracking and reforming. Currently, there is no comprehensive model for analysis of the effect of pellet pore structure on this kind of reaction. The objective of this study has been to develop a detailed model applicable to these processes, with the flexibility to analyze the effect of PSD as well as the use of designed non-uniformity and choice of other catalyst pellet properties.

2. Method of Approach

In this work, a comprehensive model has been used to assess the impact of PSD on both conversion and selectivity in a series catalytic reaction. In this series reaction, an intermediate product generated in the first reaction is desirable, while an undesirable byproduct results from a second degradation reaction where this

desirable compound transforms into waste. The evaluation of the PSD has included different combinations of micro- and macro-porosity, increasing and decreasing radial variation of the effective diffusivity, and different pellet sizes.

2.1. Description of Process Model

The reaction mechanism described in Equations (1) and (2) consists of a series reaction set taking place over a catalyst pellet. In this reaction set, the reactant $A_{(g)}$ forms the compound of interest $R_{(g)}$. However, $R_{(g)}$ degrades in a subsequent reaction to form $S_{(g)}$, an undesirable product. The compounds participating in the reactive process are in the gas phase, while the catalyst pellet is in the solid phase. All reactions have been assumed to be reversible.

$$A_{(g)} \rightleftarrows R_{(g)} \tag{1}$$

$$R_{(g)} \rightleftarrows S_{(g)} \tag{2}$$

The mass balances expressed in Equations (3) to (5) consider the effective diffusivities of each species as well as reactions through the catalyst pellet in spherical coordinates at the steady state under isothermal conditions. In these equations, D_e is the effective diffusivity of species $A_{(g)}$, $R_{(g)}$, or $S_{(g)}$, in cm^2/s; C_i represents the concentration of species $A_{(g)}$, $R_{(g)}$, or $S_{(g)}$, in mol/cm^3; r represents the catalyst radius, in cm; k_1 and k_3 are the reaction rate coefficients for the forward reactions, and k_2 and k_4 for the reverse reactions, all of them in s^{-1}.

$$\frac{1}{r^2}\frac{\mathrm{d}}{\mathrm{d}r}\left(r^2 D_e \frac{\mathrm{d}C_a}{\mathrm{d}r}\right) = k_1 C_a - k_2 C_r \tag{3}$$

$$\frac{1}{r^2}\frac{\mathrm{d}}{\mathrm{d}r}\left(r^2 D_e \frac{\mathrm{d}C_r}{\mathrm{d}r}\right) = -k_1 C_a + k_2 C_r + k_3 C_r - k_4 C_s \tag{4}$$

$$\frac{1}{r^2}\frac{\mathrm{d}}{\mathrm{d}r}\left(r^2 D_e \frac{\mathrm{d}C_s}{\mathrm{d}r}\right) = -k_3 C_r + k_4 C_s \tag{5}$$

While Equations (3) to (5) are comprehensive and need to be used when D_e varies with r, they can be simplified when D_e is constant. This special simplified version of the formulation is more efficient in numerical computation and in applying dimensionless groups that help in comparing the rates of reactions and transport steps. For constant D_e case, Equations (3) to (5) reduce to Equations (6) to (8).

$$D_e\left(\frac{2}{r}\frac{\mathrm{d}C_a}{\mathrm{d}r} + \frac{\mathrm{d}^2 C_a}{\mathrm{d}r^2}\right) = k_1 C_a - k_2 C_r \tag{6}$$

$$D_e\left(\frac{2}{r}\frac{\mathrm{d}C_r}{\mathrm{d}r} + \frac{\mathrm{d}^2 C_r}{\mathrm{d}r^2}\right) = -k_1 C_a + k_2 C_r + k_3 C_r - k_4 C_s \tag{7}$$

$$D_e\left(\frac{2}{r}\frac{\mathrm{d}C_s}{\mathrm{d}r} + \frac{\mathrm{d}^2 C_s}{\mathrm{d}r^2}\right) = -k_3 C_r + k_4 C_s \tag{8}$$

In the previous expressions, C_i and r were substituted by their related dimensionless forms [43] given in Equations (9) to (12). In these expressions, R is the pellet radius, in cm; r', C_a', C_r', and C_s' are the dimensionless forms of r, C_a,

C_r, and C_s, respectively; and C_{bulk} is the bulk concentration of $A_{(g)}$ in the surroundings of the catalyst pellet, in mol/cm^3.

$$r' = \frac{r}{R} \tag{9}$$

$$C_a' = \frac{C_a}{C_{bulk}} \cdot r' \tag{10}$$

$$C_r' = \frac{C_r}{C_{bulk}} \cdot r' \tag{11}$$

$$C_s' = \frac{C_s}{C_{bulk}} \cdot r' \tag{12}$$

After simplifications, Equations (9) to (12) reduce to the expressions depicted in Equations (13) to (15). The variable ϕ_i in Equation (16) is the Thiele modulus, which is a measure of kinetics to transport relative influence on the observed rate.

$$\frac{d^2C_a'}{dr'^2} = \phi_1 C_a' - \phi_2 C_r' \tag{13}$$

$$\frac{d^2C_r'}{dr'^2} = -\phi_1 C_a' + \phi_2 C_r' + \phi_3 C_r' - \phi_4 C_s' \tag{14}$$

$$\frac{d^2C_s'}{dr'^2} = -\phi_3 C_r' + \phi_4 C_s' \tag{15}$$

$$\phi_i = \frac{k_i R^2}{D_e} \tag{16}$$

Equations (13) to (15) were solved subjected to the boundary conditions of Equations (17) to (22).

$$r' = 0,\ C_a' = 0 \tag{17}$$

$$r' = 0,\ C_r' = 0 \tag{18}$$

$$r' = 0,\ C_s' = 0 \tag{19}$$

$$r' = 1,\ C_a' = 1 \tag{20}$$

$$r' = 1,\ C_r' = 0 \tag{21}$$

$$r' = 1,\ C_s' = 0 \tag{22}$$

To evaluate the effect of PSD on conversion and selectivity, Equations (23) to (26) are solved simultaneously. The solutions are used to evaluate the net rate of consumption of $A_{(g)}$, and the net rates of production of $R_{(g)}$ and $S_{(g)}$. These rates, shown as M_a, M_r, and M_s in mol/s, are used to calculate the conversion of the feed reactant to each product. The same parameters will be used to evaluate the effect of PSD for the cases of non-uniform D_e expressed in Equations (3) to (5).

$$M_a = \int_0^R 4\pi r^2 \left(k_1 C_a - k_2 C_r\right) dr \tag{23}$$

$$M_r = \int_0^R 4\pi r^2 \left(k_1 C_a - k_2 C_r - k_3 C_r + k_4 C_s\right) dr \tag{24}$$

$$M_s = \int_0^R 4\pi r^2 \left(-k_3 C_r + k_4 C_s\right) \mathrm{d}r \tag{25}$$

$$\text{Selectivity} = \frac{M_r}{M_a} \tag{26}$$

2.2. Effect of Porosity and Pore-Size Distribution (PSD)

To integrate the effect of PSD on the reaction performance, the catalyst's overall porosity is assumed to consist of macro and micropores. The properties and the distribution of these two pore sizes are integrated into the model parameters. Equations (27) to (28) define the ratio of macro-porosity (ϵ_m) to micro-porosity (ϵ_μ) as well as their contribution to the total porosity (ϵ). In Equation (27), n represents a parameter ranging from 0 to 1 that allows the evaluation of different PSD. The micro-porosity was varied from 0.1 to 0.5 with increments of 0.1. For each value of ϵ_μ, n was varied from 0 to a maximum value, so that ϵ was lower than 0.8.

$$\epsilon_m = n \cdot \epsilon_\mu \tag{27}$$

$$\epsilon = \epsilon_m + \epsilon_\mu \tag{28}$$

At a fixed temperature (T) and molecular weight (MW), Equations (29) to (30) are used to calculate the Knudsen diffusivities of the macro ($D_{k,m}$) and micro ($D_{k,\mu}$) pores, both in cm^2/s, using the values listed in Table 1 for the micro (a_μ) and macro (a_m) pore radii.

$$D_{k,m} = 9700 \cdot a_m \sqrt{\frac{T}{MW}} \tag{29}$$

$$D_{k,\mu} = 9700 \cdot a_\mu \sqrt{\frac{T}{MW}} \tag{30}$$

With a fixed value of bulk diffusivity (D_{AB}), the macro ($\overline{D_m}$) and micro ($\overline{D_\mu}$) diffusivities are calculated using Equations (31) to (32). The effective diffusivity is then obtained with Equation (33).

$$\frac{1}{\overline{D_m}} = \frac{1}{D_{AB}} + \frac{1}{D_{k,m}} \tag{31}$$

$$\frac{1}{\overline{D_\mu}} = \frac{1}{D_{AB}} + \frac{1}{D_{k,\mu}} \tag{32}$$

$$D_e = \epsilon_m^2 \overline{D_m} + \frac{\epsilon_\mu^2 \left(1 + 3\epsilon_m\right)}{1 - \epsilon_m} \overline{D_\mu} \tag{33}$$

2.3. Application of Non-Uniform Catalyst Pellets with Porosity Gradient

The selectivity and the reaction yield for multiple catalytic reactions depend on the pore structure inside the catalyst pellets and can be potentially improved and optimized by using pellets that are non-uniform in the pore structure. In this work,

D_e is selected as the key parameter that depends on the pore structure. Therefore, the pellets with non-uniform D_e are compared and evaluated. To explore this, three cases are considered and compared: 1) D_e increasing from the pellet center to the surface, 2) D_e decreasing from the pellet center to the surface, and 3) D_e being uniform and constant throughout the pellet. The profiles of D_e for these three cases are shown in Figure 1, where D_{eb} corresponds to the effective diffusivity of the base case with parameters listed in Table 1. In this part of the analysis, since D_e is a function of r, the general mass balances given by Equations (3) to (5) are used instead of Equations (13) to (15), which are simpler but applicable to the special case of constant D_e.

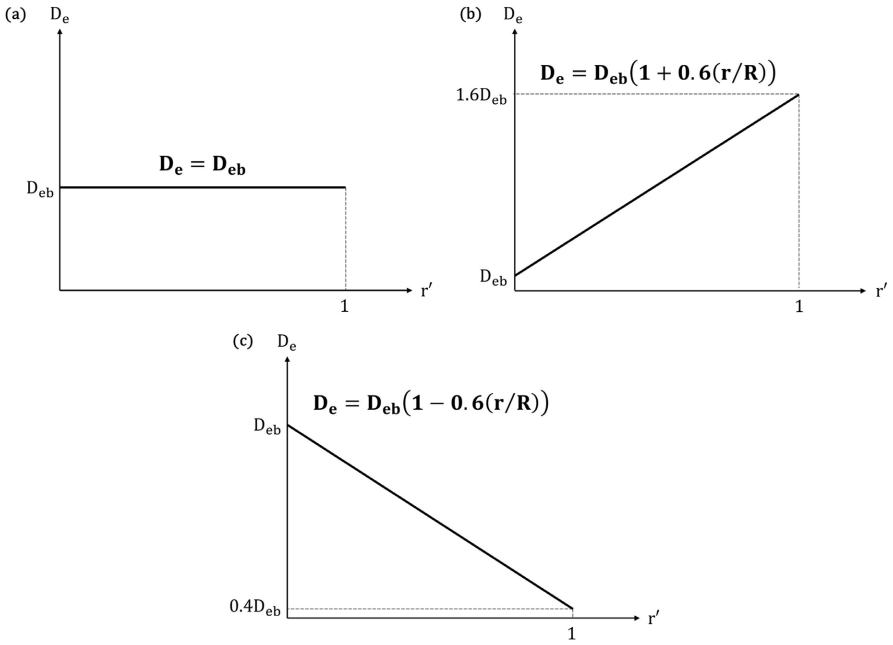

Figure 1. Uniform (a), increasing (b), and decreasing (c) variations of D_e throughout the pellet radius.

2.4. Effect of Pellet Size

The optimal ratio of macro- to micro-porosity identified in the first section was used to explore the effect of pellet size. Taking as reference the base case of Table 1, variations of 50%, 150%, and 200% with respect to the original pellet radius were implemented. As in the previous case, the effects of different diffusivity profiles shown in Figure 1 were also included in the analysis.

2.5. Process Model Parameters

Table 1 shows the full list of parameters used to perform the simulation. In the parametric study, the porosity was varied to a maximum value of 0.8 for the total porosity and 0.6 for the micro-porosity. The values for bulk diffusivity, pore diameters, pellet radius, temperature, and molecular weight were typical values for relevant industrial catalytic applications [44]-[47].

Table 1. List of parameters.

Parameter	Symbol	Value
Temperature	T	500 K
Molecular weight	MW	30
Radius of the macro-pores	a_m	2.5×10^{-8} m
Radius of the micro-pores	a_μ	1.5×10^{-9} m
Pellet radius	R	0.02 m
Bulk diffusivity	D_{AB}	5.7×10^{-5} m^2/s
Bulk concentration of $A_{(g)}$ in the surroundings of the catalyst pellet	C_{bulk}	10 mol/m^3
Reaction rate coefficient of the first forward reaction in the base case	k_{1b}	0.0065 s^{-1}
Reaction rate coefficient of the first reverse reaction in the base case	k_{2b}	0.0065 s^{-1}
Reaction rate coefficient of the second forward reaction in the base case	k_{3b}	0.00975 s^{-1}
Reaction rate coefficient of the second reverse reaction in the base case	k_{4b}	0.0039 s^{-1}
Radius of the macro-pores in the base case	a_{mb}	2.5×10^{-8} m
Radius of the micro-pores in the base case	$a_{\mu b}$	1.5×10^{-9} m
Macro-porosity in the base case	ϵ_{mb}	0.2
Micro-porosity in the base case	$\epsilon_{\mu b}$	0.5

3. Discussion of Results

3.1. Effect of Porosity and Pore-Size Distribution

Figure 2 shows the solution of Equations (3) to (5) for the case with uniform D_e, which gives the variation in the production and consumption rates of species $A_{(g)}$, $R_{(g)}$, and $S_{(g)}$ as well as the selectivity with respect to the total porosity of the pellets. In each case, fixed values of microporosities ($\epsilon_\mu = 0.1$ in Figure 2(a), 0.3 in Figure 2(b), and 0.5 in Figure 2(c)) have been used. The total porosity was varied in the ranges of 0.1 - 0.8 for the case with $\epsilon_\mu = 0.1$, 0.3 - 0.8 for the case with $\epsilon_\mu = 0.3$, and 0.5 - 0.8 for the case with $\epsilon_\mu = 0.5$, thus allowing the macro-porosity to increase up to 0.8 in each combination.

In general, the modeling findings indicate that the PSD has a significant effect on conversion and selectivity in the scale of a catalyst pellet and, therefore, in the performance of the catalytic reactor. Specifically, the results show that with larger values of micro-porosity, the net production of $R_{(g)}$ increases, but the production of the undesirable compound $S_{(g)}$ also increases. As shown in Figure 2(b) and Figure 2(c), the net production of $S_{(g)}$ doubles, and the selectivity drops from approximately 0.95 to 0.86 when the micro-porosity increases. Nevertheless, higher values of total porosity and macro-porosity increase the process yields and reduce the production of the undesired species $S_{(g)}$. This is due to the reduction of the overall intra-phase diffusion resistance as macro-porosity increases. The results

show that smaller values of ϵ_μ and larger values ϵ_m increase the overall production and consumption rates, but this trend is not entirely beneficial since it also causes higher production of the undesired compound $S_{(g)}$. Overall, the results indicate that in the case of a series reaction, the dependence of the overall conversion rate and the process selectivity are in opposite directions. Therefore, the design or the selection of a suitable catalyst structure for a particular reactor is not a simple or intuitive matter and requires an optimization process. The general model developed in this study provides a robust tool for finding the optimum structural properties of catalyst pellets for any specific reaction and process.

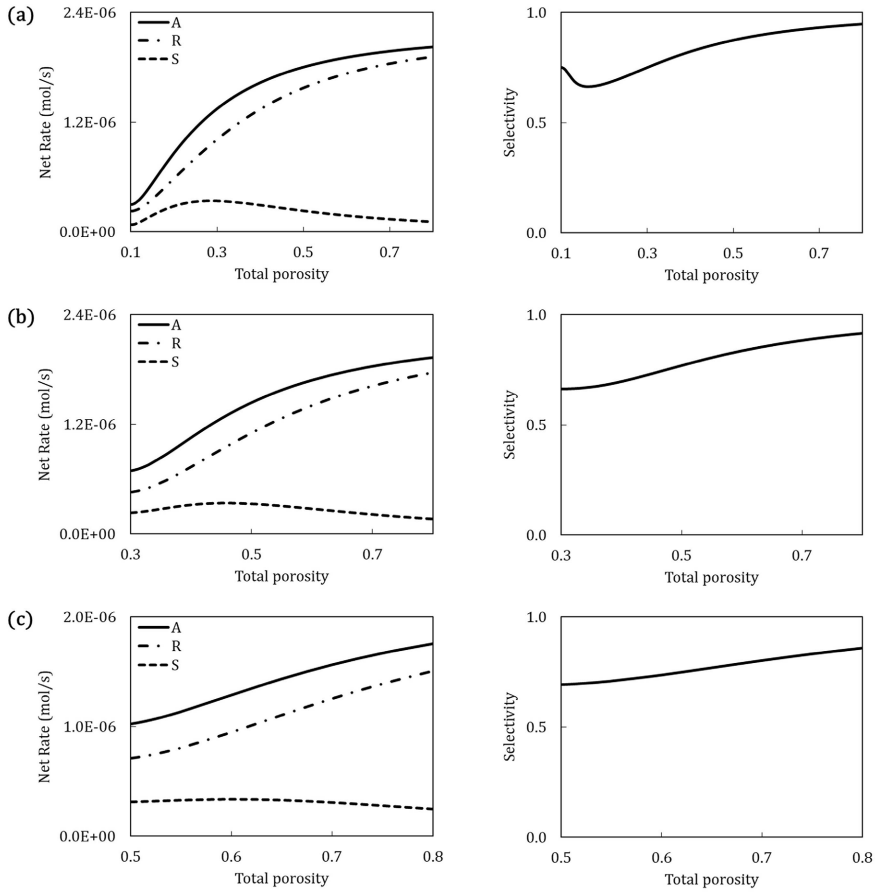

Figure 2. Effect of porosity on net rates of $A_{(g)}$, $R_{(g)}$, and $S_{(g)}$ and selectivity, including microporosities of $\epsilon_\mu = 0.1$ (a), 0.3 (b), and 0.5 (c).

It should also be noted that while the presented model focuses on the reaction kinetics in the scale of a catalyst pellet, the findings are applicable, and the formulation provides key input in the design of large-scale reactors. The model developed in this study provides a robust tool for finding the optimum structural properties of catalysts for a wide range of reactions and processes.

3.2. Non-Uniform Catalyst Pellets with Porosity Gradient

The effect of porosity and pore size on the transport of species in porous media

and, in particular, on the effective diffusivity (D_e) is well documented [30]. To utilize this effect, the model developed in this study was employed to analyze the potential advantages of catalyst pellets with a non-uniform PSD in series catalytic reactions. To explore the merits of this idea, the uniform (**Figure 1(a)**), increasing (**Figure 1(b)**), and decreasing (**Figure 1(c)**) D_e configurations were compared. Considering the dependence of D_e on porosity, each of these profiles represents a gradient of porosity and PSD in the pellet. Each case was assessed with fixed values of micro-porosity ($\epsilon_\mu = 0.1$ in **Figure 3(a)**, 0.3 in **Figure 3(b)**, and 0.5 in **Figure 3(c)**), thus allowing the total porosity to increase from 0.1, 0.3 or 0.5 to a maximum of 0.8, respectively.

The results show that the non-uniform distribution with D_e increasing from the center to the surface of the pellet gives a better rate of production of $R_{(g)}$ and a higher selectivity compared to the other two configurations. This finding is important and potentially applicable in cases where non-uniformity can be incorporated in the preparation of the catalyst pellets. The worst case is where D_e decreases from the center to the surface. This situation is not uncommon and arises when the catalytic reaction is subjected to coking and pore plugging due to impurities or undesirable solid products adsorbing on the catalyst [48]. Usually, these deactivation processes selectively reduce porosity and pore size close to the outer surface of the pellets.

The results also indicate that the effect of non-uniformity in pore distribution within the pellets is more pronounced at large values of micro-porosity. At a micro-porosity of 0.1, non-uniform D_e has the least effect on the production of the desirable compound $R_{(g)}$; the effect becomes more pronounced for higher values of micro-porosity. The production of $R_{(g)}$ and the selectivity is highest for the case with increasing D_e from the pellet core to the catalyst surface and lowest for D_e decreasing along the pellet radius. As micro-porosity increases to 0.3 (**Figure 3(b)**), the effect of non-uniform D_e becomes more pronounced. For this case, the production of $R_{(g)}$ and the selectivity are higher for the case of D_e increasing from center to surface. In highly microporous catalysts, non-uniformity can be utilized to improve performance. However, as shown in **Figure 3**, the drawback is that in all cases, the increase in micro-porosity accompanies the lowering of selectivity. This is due to the non-intuitive and complex interplay of pore distribution effects while searching for an optimum pellet configuration. Therefore, there is a need for a comprehensive model to find suitable structural properties of catalyst pellets for a given reaction set.

3.3. Effect of Pellet Size

Another important consideration in the selection of the catalyst characteristics is the pellet size. To investigate the effect of pellet size on performance in the case of series catalytic reactions, variations of 50%, 150%, and 200% in pellet size with respect to the base values given in **Table 1** were investigated. This evaluation was performed using the optimal value of $\epsilon_\mu = 0.1$ and considering the uniform

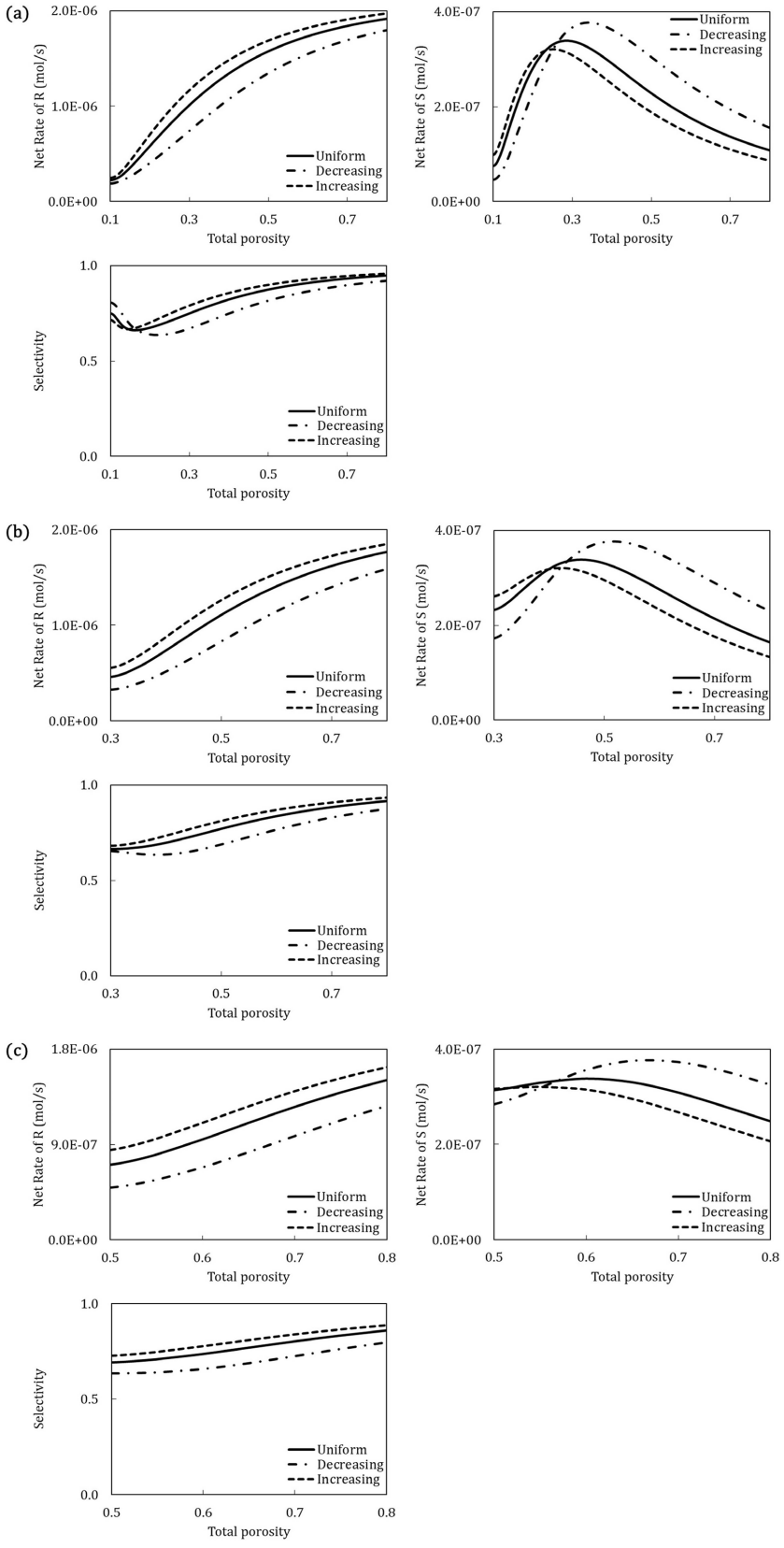

Figure 3. Effect of uniform and non-uniform profiles of D_e on the production rate of $R_{(g)}$ and $S_{(g)}$ and selectivity using microporosities of $\epsilon_\mu = 0.1$ (a), 0.3 (b), and 0.5 (c).

(Figure 4(a)), decreasing (Figure 4(b)), and increasing (Figure 4(c)) profiles of D_e. According to the results shown in Figure 4, the smallest pellet radius produced the maximum production of $R_{(g)}$ and the highest selectivity values. Conversely, increasing the pellet radius by 200% lowers the production of $R_{(g)}$ and selectivity, even falling below half of the values attained when the radius was reduced by 50%. The best results were obtained when the total porosity was 0.8 ($\epsilon_\mu = 0.1$, $\epsilon_m = 0.7$). In general, the increase in the overall diffusional resistance by using larger pellets has a detrimental effect on the catalyst performance in the case of series reactions under the conditions studied.

The observed trend on the effect of pellet size for series reactions is particularly important and non-intuitive, considering that diffusion can be beneficial and can be used to suppress the formation of undesirable products and enhance selectivity in some other multiple reactions. While smaller pellet sizes give better performance, there are limitations to lowering the pellet size in packed bed reactors due to factors not related to reaction kinetics. Some of these factors include the effect of pellet size on pressure drop, the mechanical attrition of the pellets in the packed reactors, and other considerations beyond the scope of this work. The selectivity trends for the case of D_e decreasing toward the surface are quite different from the others (Figure 4(b)). However, based on the results of the previous section, this kind of non-uniform distribution is not a good choice for the series reactions considered here.

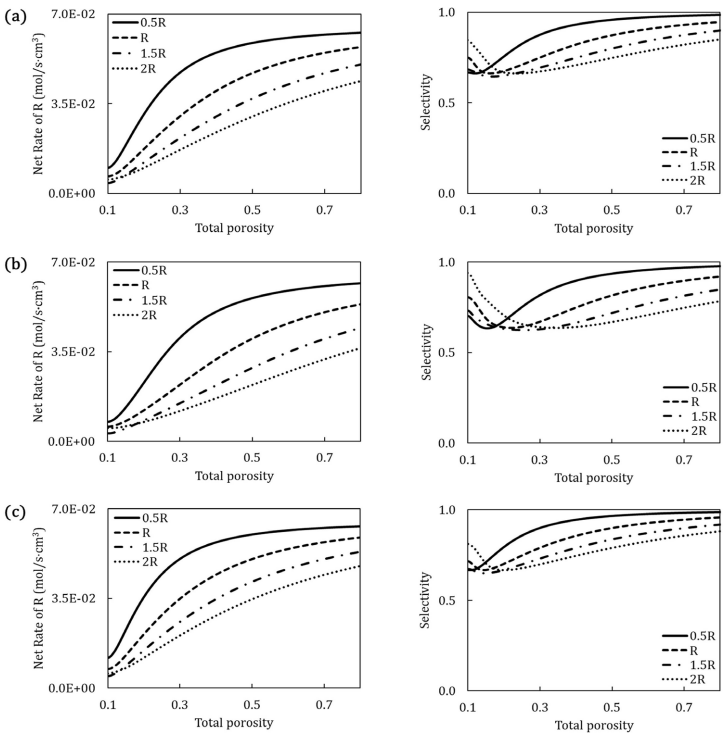

Figure 4. Effect of pellet size on the production rate of $R_{(g)}$ and selectivity using the uniform (a), decreasing (b), and increasing (c) profiles of D_e. Variations of 50%, 150%, and 200% with respect to the original R value were considered in the analysis. The micro-porosity was fixed at $\epsilon_\mu = 0.1$ in all cases.

4. Conclusion

In reacting systems for multiple reactions that produce both desirable and undesirable products, two factors determine the overall performance of the catalyst: conversion and selectivity. These performance factors are sensitive to the physical properties of the porous catalyst pellets and the pore structure. The case of series multiple reactions with the desirable product being intermediate in the series is investigated over a wide range of catalyst properties. Results show that when the physical properties are varied, the trends of improvement in conversion and selectivity are often in opposite directions. A major conclusion is that an optimum catalyst design and selection requires a detailed process modeling approach to determine the desired balance between conversion and selectivity. The comprehensive model developed in this study is a robust tool that fills this needed gap. It is useful for the optimization process in determining the effects of pellet size, overall porosity, and the distribution of pore size between macro and micro-pores in catalyst pellets for series catalytic reactions.

Acknowledgements

The authors of this study acknowledge the support of the Office of Research and Innovation of the Universidad Centroamericana "José Simeón Cañas". Likewise, we appreciate the support of Mario Zetino Duarte, Carmen Menjívar, Henry Menéndez, and Hazel Ramos.

Conflicts of Interest

The authors declare no known competing financial interests or personal relationships that could have appeared to influence the results reported in this paper.

References

[1] Lok, C.M. (2018) Structure and Performance of Selective Hydrogenation Catalysts. In: *Hydrogenation*, de Gruyter, 1-18. https://doi.org/10.1515/9783110545210-001

[2] Coker, A. (2001) Modeling of Chemical Kinetics and Reactor Design. 2nd Edition, Gulf Professional Publishing.

[3] Helfferich, F.G. (2004) Preface. In: *Comprehensive Chemical Kinetics*, Elsevier, 3-10. https://doi.org/10.1016/s0069-8040(04)80002-5

[4] Kiperman, S.L. (1986) Some Problems of Chemical Kinetics in Heterogeneous Hydrogenation Catalysis. In: *Studies in Surface Science and Catalysis*, Elsevier, 1-52. https://doi.org/10.1016/s0167-2991(08)65347-1

[5] Murzin, D.Y. (2022) Chemical Reaction Technology. 2nd Edition, De Gruyter. https://doi.org/10.1515/9783110712551

[6] Newson, E. (1975) Catalyst Deactivation Due to Pore-Plugging by Reaction Products. *Industrial & Engineering Chemistry Process Design and Development*, **14**, 27-33. https://doi.org/10.1021/i260053a005

[7] Speight, J.G. (2014) The Chemistry and Technology of Petroleum. 5th Edition, Taylor & Francis Group.

[8] Fogler, H.S. (2020) Elements of Reaction Engineering. 6th Edition, Pearson Education.

[9] Fu, P.P. and Harvey, R.G. (1978) Dehydrogenation of Polycyclic Hydroaromatic Compounds. *Chemical Reviews*, **78**, 317-361. https://doi.org/10.1021/cr60314a001

[10] Ponec, V. (1975) Selectivity in Catalysis by Alloys. *Catalysis Reviews*, **11**, 41-70. https://doi.org/10.1080/01614947508079981

[11] Ponec, V. and Bond, G. (1995) Catalysis by Metals and Alloys. Elsevier Science.

[12] Speight, J.G. (2019) Handbook of Industrial Hydrocarbon Processes. 2nd Edition, Gulf Professional Publishing.

[13] Vora, B.V. (2012) Development of Dehydrogenation Catalysts and Processes. *Topics in Catalysis*, **55**, 1297-1308. https://doi.org/10.1007/s11244-012-9917-9

[14] Krishna, R. and Wesselingh, J.A. (1997) The Maxwell-Stefan Approach to Mass Transfer. *Chemical Engineering Science*, **52**, 861-911. https://doi.org/10.1016/s0009-2509(96)00458-7

[15] Yao, J., Huang, Y. and Wang, H. (2010) Controlling Zeolite Structures and Morphologies Using Polymer Networks. *Journal of Materials Chemistry*, **20**, 9827-9831. https://doi.org/10.1039/c0jm01003k

[16] Triantafillidis, C., Elsaesser, M.S. and Hüsing, N. (2013) Chemical Phase Separation Strategies Towards Silica Monoliths with Hierarchical Porosity. *Chemical Society Reviews*, **42**, 3833-3846. https://doi.org/10.1039/c3cs35345a

[17] Petkovich, N.D. and Stein, A. (2013) Controlling Macro and Mesostructures with Hierarchical Porosity through Combined Hard and Soft Templating. *Chemical Society Reviews*, **42**, 3721-3739. https://doi.org/10.1039/c2cs35308c

[18] Ye, G., Duan, X., Zhu, K., Zhou, X., Coppens, M. and Yuan, W. (2015) Optimizing Spatial Pore-Size and Porosity Distributions of Adsorbents for Enhanced Adsorption and Desorption Performance. *Chemical Engineering Science*, **132**, 108-117. https://doi.org/10.1016/j.ces.2015.04.024

[19] Sun, J., Shan, Z., Maschmeyer, T. and Coppens, M. (2003) Synthesis of Bimodal Nanostructured Silicas with Independently Controlled Small and Large Mesopore Sizes. *Langmuir*, **19**, 8395-8402. https://doi.org/10.1021/la0351156

[20] Christensen, C.H., Johannsen, K., Schmidt, I. and Christensen, C.H. (2003) Catalytic Benzene Alkylation over Mesoporous Zeolite Single Crystals: Improving Activity and Selectivity with a New Family of Porous Materials. *Journal of the American Chemical Society*, **125**, 13370-13371. https://doi.org/10.1021/ja037063c

[21] Van Donk, S., Janssen, A.H., Bitter, J.H. and de Jong, K.P. (2003) Generation, Characterization, and Impact of Mesopores in Zeolite Catalysts. *Catalysis Reviews—Science and Engineering*, **45**, 297-319. https://doi.org/10.1081/CR-120023908

[22] Choi, M., Cho, H.S., Srivastava, R., Venkatesan, C., Choi, D. and Ryoo, R. (2006) Amphiphilic Organosilane-Directed Synthesis of Crystalline Zeolite with Tunable Mesoporosity. *Nature Materials*, **5**, 718-723. https://doi.org/10.1038/nmat1705

[23] Groen, J.C., Zhu, W., Brouwer, S., Huynink, S.J., Kapteijn, F., Moulijn, J.A., *et al.* (2006) Direct Demonstration of Enhanced Diffusion in Mesoporous ZSM-5 Zeolite Obtained via Controlled Desilication. *Journal of the American Chemical Society*, **129**, 355-360. https://doi.org/10.1021/ja065737o

[24] Wang, J., Groen, J.C., Yue, W., Zhou, W. and Coppens, M. (2007) Single-Template Synthesis of Zeolite ZSM-5 Composites with Tunable Mesoporosity. *Chemical Communications*, **44**, 4653-4655. https://doi.org/10.1039/b708822a

[25] Wang, G. and Coppens, M. (2010) Rational Design of Hierarchically Structured Porous Catalysts for Autothermal Reforming of Methane. *Chemical Engineering Science*, **65**, 2344-2351. https://doi.org/10.1016/j.ces.2009.09.079

[26] Zhu, L., Ma, W. and Luo, Z. (2018) Influence of Distributed Pore Size and Porosity on MTO Catalyst Particle Performance: Modeling and Simulation. *Chemical Engineering Research and Design*, **137**, 141-153. https://doi.org/10.1016/j.cherd.2018.07.005

[27] Wang, G. and Coppens, M. (2008) Calculation of the Optimal Macropore Size in Nanoporous Catalysts and Its Application to Denox Catalysis. *Industrial & Engineering Chemistry Research*, **47**, 3847-3855. https://doi.org/10.1021/ie071550+

[28] Shimada, H., Kurita, M., Sato, T., Yoshimura, Y., Kawakami, T., Yoshitomi, S., *et al.* (1984) Effects of Pore Size Distribution on the Catalytic Performance for Coal Liquefaction. I. The Activity and Selectivity of the Catalyst. *Bulletin of the Chemical Society of Japan*, **57**, 2000-2004. https://doi.org/10.1246/bcsj.57.2000

[29] Rao, S.M. and Coppens, M. (2012) Increasing Robustness against Deactivation of Nanoporous Catalysts by Introducing an Optimized Hierarchical Pore Network—Application to Hydrodemetalation. *Chemical Engineering Science*, **83**, 66-76. https://doi.org/10.1016/j.ces.2011.11.044

[30] Gheorghiu, S. and Coppens, M. (2004) Optimal Bimodal Pore Networks for Heterogeneous Catalysis. *AIChE Journal*, **50**, 812-820. https://doi.org/10.1002/aic.10076

[31] Wang, G., Johannessen, E., Kleijn, C.R., de Leeuw, S.W. and Coppens, M. (2007) Optimizing Transport in Nanostructured Catalysts: A Computational Study. *Chemical Engineering Science*, **62**, 5110-5116. https://doi.org/10.1016/j.ces.2007.01.046

[32] Carberry, J.J. (1962) The Micro-Macro Effectiveness Factor for the Reversible Catalytic Reaction. *AIChE Journal*, **8**, 557-558. https://doi.org/10.1002/aic.690080428

[33] Örs, N. and Doğu, T. (1979) Effectiveness of Bidisperse Catalysts. *AIChE Journal*, **25**, 723-725. https://doi.org/10.1002/aic.690250422

[34] Doğu, G. and Doğu, T. (1980) A General Criterion to Test the Importance of Diffusion Limitations in Bidisperse Porous Catalysts. *AIChE Journal*, **26**, 287-288. https://doi.org/10.1002/aic.690260212

[35] Kulkarni, B.D., Jayaraman, V.K. and Doraiswamy, L.K. (1981) Effectiveness Factors in Bidispersed Catalysts: The General Nth Order Case. *Chemical Engineering Science*, **36**, 943-945. https://doi.org/10.1016/0009-2509(81)85050-6

[36] Loewenberg, M. (1994) Diffusion-Controlled, Heterogeneous Reaction in a Material with a Bimodal Poresize Distribution. *The Journal of Chemical Physics*, **100**, 7580-7589. https://doi.org/10.1063/1.466851

[37] Doğu, T. (1998) Diffusion and Reaction in Catalyst Pellets with Bidisperse Pore Size Distribution. *Industrial & Engineering Chemistry Research*, **37**, 2158-2171. https://doi.org/10.1021/ie970613t

[38] Martínez, V.A.C. and Shadman, F. (2020) Improving the Performance of Fixed-Bed Catalytic Reactors by Innovative Catalyst Distribution. *Journal of Applied Mathematics and Physics*, **8**, 672-683. https://doi.org/10.4236/jamp.2020.84052

[39] Martínez, V. and Shadman, F. (2022) Non-Uniform Catalyst Distribution in Fixed-Bed Reactors to Improve Dehydrogenation Processes. *Chemical Engineering Journal Advances*, **10**, Article 100254. https://doi.org/10.1016/j.ceja.2022.100254

[40] Hegedus, L.L. (1980) Catalyst Pore Structures by Constrained Nonlinear Optimization. *Industrial & Engineering Chemistry Product Research and Development*, **19**, 533-537. https://doi.org/10.1021/i360076a010

[41] Pereira, C.J., Kubsh, J.E. and Hegedus, L.L. (1988) Computer-Aided Design of Catalytic Monoliths for Automobile Emission Control. *Chemical Engineering Science*, **43**, 2087-2094. https://doi.org/10.1016/0009-2509(88)87088-x

[42] Beeckman, J.W. and Hegedus, L.L. (1991) Design of Monolith Catalysts for Power Plant Nitrogen Oxide (No.+-.) Emission Control. *Industrial & Engineering Chemistry Research*, **30**, 969-978. https://doi.org/10.1021/ie00053a020

[43] Rice, R. and Do, D. (1995) Applied Mathematics and Modeling for Chemical Engineers. Wiley.

[44] Armatas, G.S. (2006) Determination of the Effects of the Pore Size Distribution and Pore Connectivity Distribution on the Pore Tortuosity and Diffusive Transport in Model Porous Networks. *Chemical Engineering Science*, **61**, 4662-4675. https://doi.org/10.1016/j.ces.2006.02.036

[45] Cui, C.L., Schweich, D. and Villermaux, J. (1989) Influence of Pore Diameter Distribution on the Determination of Effective Diffusivity in Porous Particles. *Chemical Engineering and Processing*: *Process Intensification*, **26**, 121-126. https://doi.org/10.1016/0255-2701(89)90004-4

[46] Mezedur, M.M., Kaviany, M. and Moore, W. (2002) Effect of Pore Structure, Randomness and Size on Effective Mass Diffusivity. *AIChE Journal*, **48**, 15-24. https://doi.org/10.1002/aic.690480104

[47] Reid, R.C., Prausnitz, J.M. and Poling, B.E. (1987) The Properties of Gases and Liquids. 4th Edition, McGraw-Hill.

[48] Beuther, H., Larson, O.A. and Perrotta, A.J. (1980) The Mechanism of Coke Formation on Catalysts. In: *Studies in Surface Science and Catalysis*, Elsevier, 271-282. https://doi.org/10.1016/s0167-2991(08)65236-2

List of Symbols

ϵ	Porosity
ϵ_m	Macro-porosity
ϵ_{mb}	Macro-porosity in the base case
ϵ_μ	Micro-porosity
$\epsilon_{\mu b}$	Micro-porosity in the base case
ϕ_1	Thiele modulus of the first direct reaction
ϕ_2	Thiele modulus of the first forward reaction
ϕ_3	Thiele modulus of the second direct reaction
ϕ_4	Thiele modulus of the second forward reaction
ϕ_i	Thiele modulus
a_m	Radius of the macro-pores, cm
a_{mb}	Radius of the macro-pores in the base case, cm
a_μ	Radius of the micro-pores, cm
$a_{\mu b}$	Radius of the micro-pores, cm
C_a	Concentration of $A_{(g)}$, mol/cm^3
C'_a	Dimensionless concentration of $A_{(g)}$
C_{bulk}	Bulk concentration of $A_{(g)}$, mol/cm^3
C_i	Concentration of gaseous species, mol/cm^3
C_r	Concentration of $R_{(g)}$, mol/cm^3
C'_r	Dimensionless concentration of $R_{(g)}$
C_s	Concentration of $S_{(g)}$, mol/cm^3
C'_s	Dimensionless concentration of $S_{(g)}$
D_{AB}	Bulk diffusivity, cm^2/s
D_e	Effective diffusivity of species $A_{(g)}$, $R_{(g)}$, or $S_{(g)}$, cm^2/s
D_{eb}	Diffusivity of the base case, cm^2/s
$D_{k,m}$	Knudsen diffusivity in the macro-pores, cm^2/s
$D_{k,\mu}$	Knudsen diffusivity in the micro-pores, cm^2/s
$\overline{D_m}$	Macro-diffusivity, cm^2/s
$\overline{D_\mu}$	Micro-diffusivity, cm^2/s
k_1	Rate coefficient of the first forward reaction, s^{-1}
k_{1b}	Rate coefficient of the first forward reaction in the base case, s^{-1}
k_2	Rate coefficient of the first reverse reaction, s^{-1}
k_{2b}	Rate coefficient of the first reverse reaction in the base case, s^{-1}
k_3	Rate coefficient of the second forward reaction, s^{-1}
k_{3b}	Rate coefficient of the second forward reaction in the base case, s^{-1}
k_4	Rate coefficient of the second reverse reaction, s^{-1}
k_{4b}	Rate coefficient of the second reverse reaction in the base case, s^{-1}
M_a	Consumption rate of species $A_{(g)}$, mol/s
M_r	Production rate of species $R_{(g)}$, mol/s
M_s	Production rate of species $S_{(g)}$, mol/s
MW	Molecular weight
n	Parametric variable

PSD	Pore-Size Distribution
r	Coordinate on the r-axis, cm
r'	Dimensionless r-coordinate, cm
R	Catalyst radius, cm
T	Temperature, K